Implementation of Constitutive Model for Thermoplastics with Some Preliminary Results

Torodd Berstad*
SINTEF Materials and Chemistry,
NO–7491 Trondheim, Norway

Odd Sture Hopperstad, Arild H. Clausen
Structural Impact Laboratory (SIMLab),
Department of Structural Engineering,
Norwegian University of Science and Technology,
NO–7491 Trondheim, Norway

Håvar Ilstad, Bjørn Melve
Statoil ASA
NO-7005 Trondheim, Norway

Abstract

This paper presents an implementation of a material model for thermoplastics. Such materials have a quite complex behavior involving large elastic and plastic deformations, strong viscous and temperature effects, possible true stress softening and deformation-induced anisotropy. The demand of reliable constitutive models for thermoplastics is increasing, and a promising approach is due to Haward and Thackray (1968), who separated the response in two processes: one flow process related to motion of polymer chain segments, and one extendable spring based on the conventional theory of elastomers. Several researchers have extended the Haward and Thackray model, and in particular, the group headed by Boyce at MIT has worked with modeling of polymers for years. The implementation in this paper is mainly based on a paper by Boyce et al. (2000). Recognizing the large elastic deformations in polymers, we have used a framework with a Neo-Hookean hyperelastic material description. The semi-implicit stress update algorithm is as proposed by Moran et al. (1990). Predictions using the implemented model is compared with results from uniaxial tension and compression tests on polypropylene. The agreement is satisfactory in both cases of loading, as the main features of the force-deformation curve and yield stress difference in compression and tension are reproduced by the model.

Introduction

Many material scientists define three classes of polymers: Thermoplastics, thermosets and rubbers. The physical structure of a thermoplastic consists of long molecule chains which are very loosely connected with each other. The chains are therefore free to slide and rotate relative to their neighbor chains. Considering rubbers and in particular thermosets, however, there are several chemical bonds, or cross-links, between the chains, and these connectors provide mechanical properties different from those observed for thermoplastics.

Thermoplastics, in particular, turn out to be difficult to model in FE codes. This class of materials has usually a very ductile behavior involving large elastic and plastic strains.

* Corresponding author.
E-mail: torodd.berstad@sintef.no

Moreover, the relative movement of the chains is a thermal activated process with viscous characteristics, and the mechanical properties are therefore strongly dependent on temperature and strain rate. A third feature is the pressure sensitivity, resulting in different behavior in tension and compression. Further, thermoplastics experience often strain softening after initial yielding and cold drawing at almost constant stress, corresponding to straightening of the molecule chains. The consequence is a deformation-induced anisotropy. Summing up, there are several challenges in polymer modeling which are not relevant for other materials such as metals and ceramics.

Thermoplastics have several attractive properties: They are light, cheap, easy to form, ductile and – at least in some environments – sustainable. Therefore, the interest for using thermoplastics in load-carrying parts of different structures is increasing, and so is the need for reliable constitutive models for thermoplastics in FE codes. Despite substantial research effort during the last decades, Du Bois et al. (2006) claim that existing models for thermoplastics in LS-DYNA still need improvement, whilst, on the other hand, they report that there exist user-friendly models with satisfactory accuracy for rubber-like materials in LS-DYNA.

Predictions from the model is compared with results from uniaxial tension and compression tests on polypropylene BA212. Polypropylene has a thermoplastic market share of about 20% in Europe, and has low density and price compared with most other thermoplastics (Mills, 2005). Moreover, polypropylene have rather high stiffness and strength, but fracture may be a problem (McCrum et al., 1997). A possible application of this material is as a protection cover around offshore pipelines, preventing the tube against impact during trawling. Numerical analyses of this problem, of course, demand a material model covering large deformations, high strain-rates, cyclic loading and preferably also fracture. With this motivation, a joint project was established between Statoil and NTNU in order to evaluate candidate models well-suited for implementation in explicit FE codes.

Material Model

Several researchers within the field, including e.g. Meijer and Govaert (2005), Buckley and Jones (1995), and Boyce et al. (1988), point out that an article written by Haward and Thackray (1968) was a pioneering work. Haward and Thackray assumed that the total stress was the sum of two contributions, see Fig. 1. In accordance with the notation established by Boyce and co-workers in several publications, these two contributions are denoted A and B, respectively:

A. An inter-molecular barrier to deformation related to relative movement between molecules.
B. An evolving anisotropic resistance related to straightening of the molecule chains.

The model which is implemented and presented in this paper is mainly based on the framework suggested by Boyce et al. (2000). Going back to the original work by Haward and Thackray (1968), they considered the uniaxial case only. The extension to a full 3D formulation was proposed by Boyce et al. (1988). Moreover, Boyce and co-workers have during a period of 20 years changed or further developed the parts of the original model. Haward and Thackray (1968) used an Eyring model to represent the dashpot in Fig.1, whilst Boyce et al. (2000) employed the double-kink model of Argon (1973) instead. Part B of the model, describing the resistance associated with straightening of the molecules, contained originally a one-dimensional Langevin

spring (Haward and Thackray, 1968), which was generalized to 3D with the eight-chain model by Arruda and Boyce (1993).

The main structure of the model presented by Boyce et al. (2000) is kept in this paper. Recognizing the large elastic deformations occurring for polymers, a formulation based on a Neo-Hookean material is here selected for describing the spring in resistance A in Fig. 1.

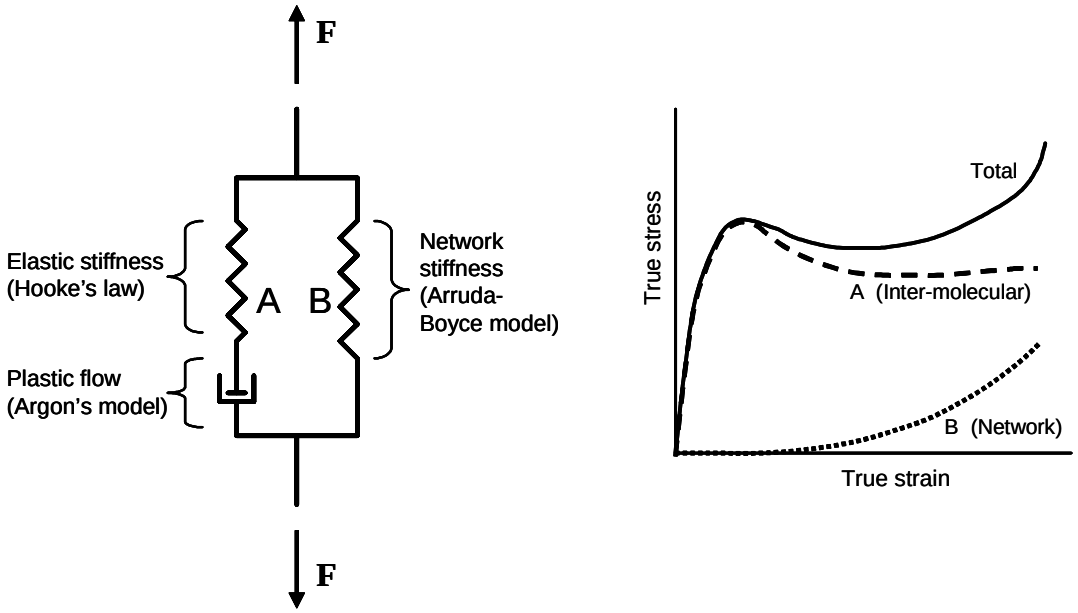

Figure 1: Stress decomposition in inter-molecular and network contributions.

Referring to Fig. 1, it is assumed that the deformation gradient tensor is the same for the two resistances (Part A and B)

$$\mathbf{F} = \mathbf{F}_A = \mathbf{F}_B \tag{1}$$

while the Cauchy stress tensor for the system is assumed to be the sum of the Cauchy stress tensors for the two parts

$$\boldsymbol{\sigma} = \boldsymbol{\sigma}_A + \boldsymbol{\sigma}_B \tag{2}$$

Part A – Inter-molecular Resistance

The deformation is decomposed into elastic and plastic parts, $\mathbf{F}_A = \mathbf{F}_A^e \cdot \mathbf{F}_A^p$, where it is assumed that the intermediate configuration $\bar{\Omega}_A$ defined by $\mathbf{F}_A^p$ is invariant to rigid body rotations of the current configuration. The velocity gradient in the current configuration Ω is defined by

$$\mathbf{L}_A = \dot{\mathbf{F}}_A \cdot \mathbf{F}_A^{-1} = \mathbf{L}_A^e + \mathbf{L}_A^p \tag{3}$$

Owing to the decomposition, $\mathbf{F}_A = \mathbf{F}_A^e \cdot \mathbf{F}_A^p$, the elastic and plastic rate-of-deformation and spin tensors are defined by

$$\begin{aligned} \mathbf{L}_A^e &= \mathbf{D}_A^e + \mathbf{W}_A^e = \dot{\mathbf{F}}_A^e \cdot (\mathbf{F}_A^e)^{-1} \\ \mathbf{L}_A^p &= \mathbf{D}_A^p + \mathbf{W}_A^p = \mathbf{F}_A^e \cdot \dot{\mathbf{F}}_A^p \cdot (\mathbf{F}_A^p)^{-1} \cdot (\mathbf{F}_A^e)^{-1} = \mathbf{F}_A^e \cdot \bar{\mathbf{L}}_A^p \cdot (\mathbf{F}_A^e)^{-1} \end{aligned} \tag{4}$$

where $\bar{\mathbf{L}}_A^p = \dot{\mathbf{F}}_A^p \cdot (\mathbf{F}_A^p)^{-1}$. The Neo-Hookean material represents an extension of Hooke's law to large elastic deformations and may be chosen for the elastic part of the deformation when the elastic behavior is assumed to be isotropic, viz.

$$\boldsymbol{\tau}_A = \lambda_0 \ln J_A^e \, \mathbf{I} + \mu_0 (\mathbf{B}_A^e - \mathbf{I}) \tag{5}$$

where $\boldsymbol{\tau}_A = J_A \boldsymbol{\sigma}_A$ is the Kirchhoff stress tensor of Part A and $J_A^e = \sqrt{\det \mathbf{B}_A^e} = J_A$ is the Jacobian determinant. The elastic left Cauchy-Green deformation tensor is given by $\mathbf{B}_A^e = \mathbf{F}_A^e \cdot \mathbf{F}_A^{eT}$.

The flow rule is defined by

$$\mathbf{L}_A^p = \dot{\gamma}_A^p \mathbf{N}_A \tag{6}$$

where

$$\mathbf{N}_A = \frac{1}{\sqrt{2}\,\tau_A} \boldsymbol{\tau}_A^{dev}, \quad \tau_A = \sqrt{\frac{1}{2} \mathrm{tr}\left(\boldsymbol{\tau}_A^{dev}\right)^2} \tag{7}$$

and $\boldsymbol{\tau}_A^{dev}$ is the stress deviator. The rate of flow is taken to be a thermally activated process

$$\dot{\gamma}_A^p = \dot{\gamma}_{0A} \exp\left[-\frac{\Delta G \left(1 - \tau_A / s\right)}{k\theta} \right] \tag{8}$$

where $\dot{\gamma}_{0A}$ is a pre-exponential factor, ΔG is the energy barrier to flow, s is the shear resistance, k is the Boltzmann constant and θ is the absolute temperature. The shear resistance s is assumed to depend on the stress triaxiality σ^*, viz.

$$s = s\left(\sigma^*\right), \quad \sigma^* = \frac{\operatorname{tr}\boldsymbol{\sigma}_A}{3\sqrt{3}\tau_A} \tag{9}$$

The exact dependence is given by a user-defined load curve, which is linear between the shear resistances in compression and tension. These resistances are denoted s_c and s_t, respectively.

Part B – Network Resistance

The network resistance is assumed to be nonlinear elastic with deformation gradient $\mathbf{F}_B = \mathbf{F}_B^N$, i.e. any viscoplastic deformation of the network is neglected. The stress-stretch relation is defined by

$$\boldsymbol{\tau}_B = \frac{nk\theta}{3}\frac{\sqrt{N}}{\bar{\lambda}_N}\mathcal{L}^{-1}\left(\frac{\bar{\lambda}_N}{\sqrt{N}}\right)(\bar{\mathbf{B}}_B^N - \bar{\lambda}_N^2\mathbf{I}) \tag{10}$$

where $\boldsymbol{\tau}_B = J_B\boldsymbol{\sigma}_B$ is the Kirchhoff stress for Part B, n is the chain density and N the number of 'rigid links' between entanglements. In accordance with Boyce et al. (2000), the product $nk\theta$ is denoted C_R herein. Moreover, $\mathcal{L}^{-1}$ is the inverse Langevin function, $\mathcal{L}(\beta) = \coth\beta - 1/\beta$, and further

$$\bar{\mathbf{B}}_B^N = \bar{\mathbf{F}}_B^N \cdot \bar{\mathbf{F}}_B^{NT}, \quad \bar{\mathbf{F}}_B^N = J_B^{-1/3}\mathbf{F}_B^N, \quad J_B = \det\mathbf{F}_B^N, \quad \bar{\lambda}_N = \left[\frac{1}{3}\operatorname{tr}\bar{\mathbf{B}}_B^N\right]^{\frac{1}{2}} \tag{11}$$

The model has been implemented into LS-DYNA using a semi-implicit stress-update scheme (Moran et al., 1990), and is available for the explicit solver only.

Uniaxial Material Tests

Test specimens for uniaxial tension and compression tests were machined from a lump of the polypropylene quality BA212, which is produced by Borealis. The geometry of the specimens is shown in Fig. 2. The tests were conducted under displacement control, and the cross-head velocity of the servohydraulic testing machine was 4.0 mm/min in tension and 1.13 mm/min in compression. These velocities were kept constant during the entire test, and they correspond to a nominal strain rate of 0.002 s^{-1} in both tension and compression. During the test, the force and elongation (tension) or contraction (compression) of the coupon were registered. Four tension tests and two compression tests were performed, and there was hardly no scatter between parallel tests. Thus, one representative test of each type is presented in this paper.

LS-DYNA Simulation of Laboratory Tests

The two specimens depicted in Fig. 2 were modeled in LS-DYNA using 8-node brick elements, see Fig. 3. As in the laboratory test, the specimen was deformed by applying a constant velocity with value as defined above at one end of the specimen, while the other end was fixed. The material coefficients used in the simulations are given in Table 1.

Table 1: Parameters in material model

E [MPa]	ν	$\dot{\gamma}_{0A}$ [s^{-1}]	ΔG [J]	k [J/K]	C_R [MPa]	N	θ [K]	s_t [MPa]	s_c [MPa]
1200	0.49	$6.67 \cdot 10^{6}$	$2.17 \cdot 10^{-19}$	$1.38 \cdot 10^{-23}$	4	6	293	25	46

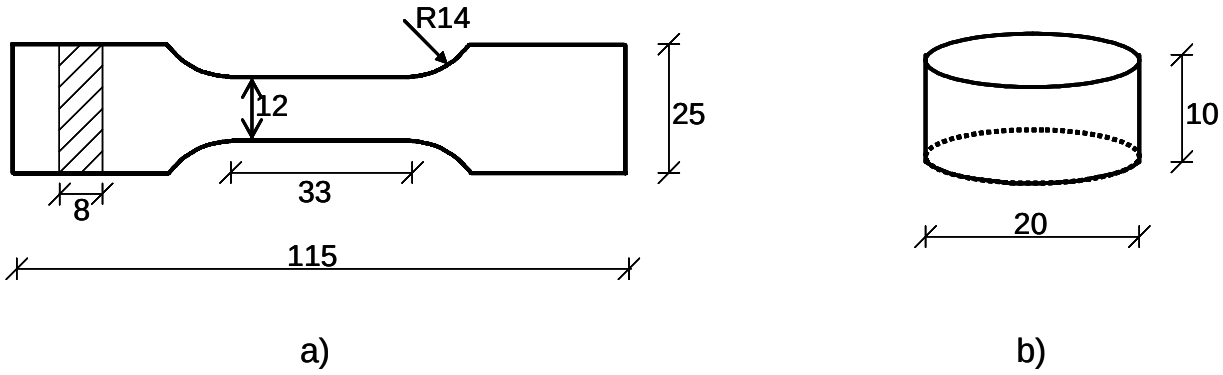

Figure 2: a) Tension test coupon b) Compression test coupon (Measures in mm)

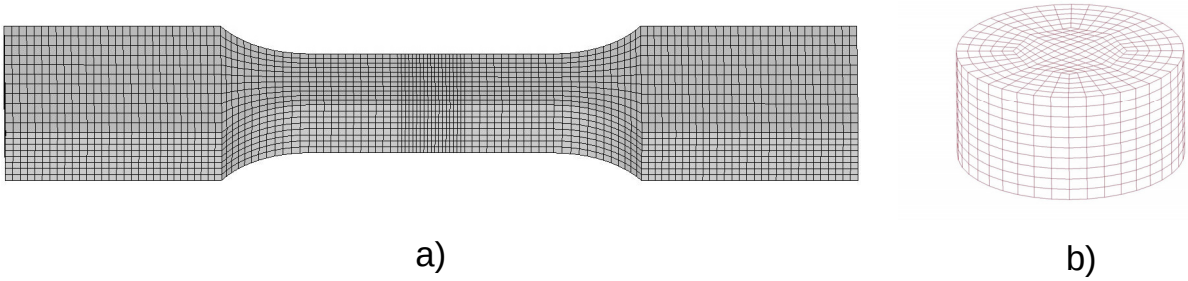

Figure 3: LS-DYNA model of coupons a) Tension test b) Compression test

Results From Laboratory Tests and Numerical Simulations

Figure 4a) and b) show force-displacement curves in tension and compression, respectively, from the experimental tests and LS-DYNA predictions. In both cases, the first phase of the deformation process, i.e. the initial elastic part and the subsequent yielding, is well represented by the numerical model. Continuing to large deformations, some deviation between test and LS-DYNA results is observed. Considering compression, see Fig. 4b), the main tendency in the test,

involving a force plateau close to 20 kN followed by an increase in force, is handled qualitatively well by the model. The agreement between the two curves in tension, see Fig. 4a), is also satisfactory. The simulation does not predict a constant force in the cold drawing region of the force-displacement curve, and the fluctuations are caused by small localization effects in the specimen which are moderated by the stress increase associated with resistance B in Fig. 1. At the present stage of research, any failure criterion is neither considered nor implemented, and the model is therefore not able to predict the failure as observed in the tests.

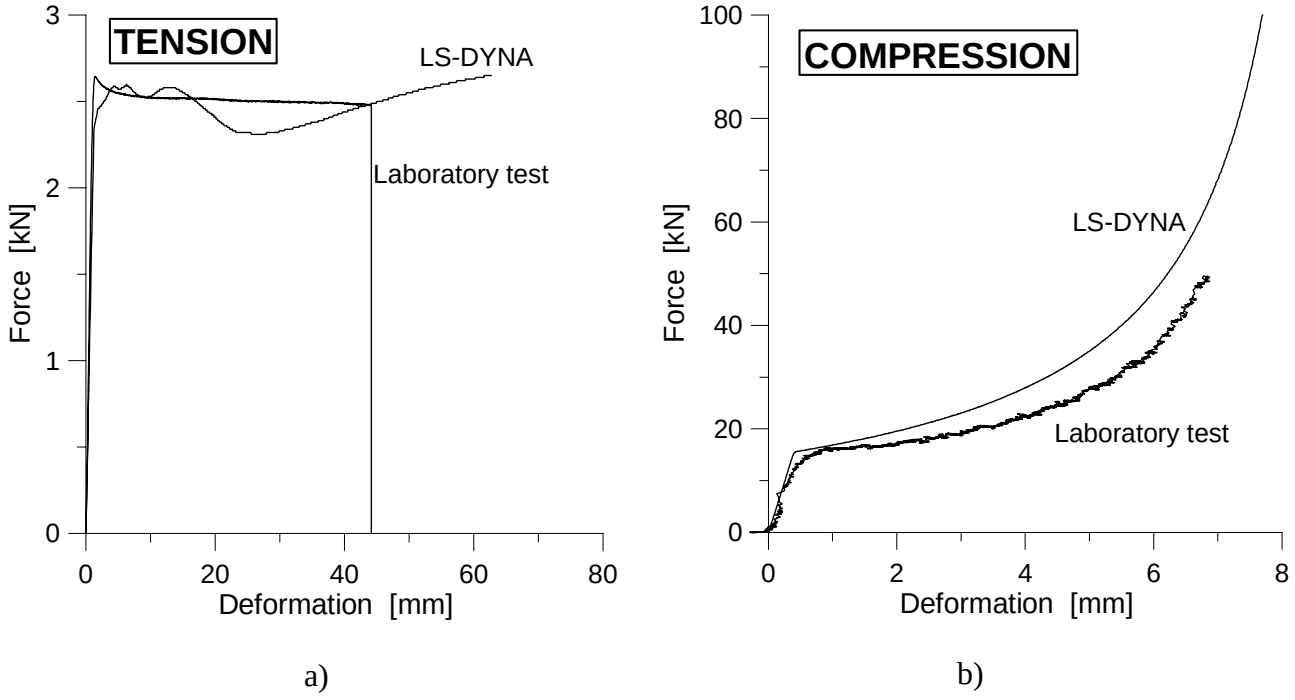

Figure 4: Force-displacement curves a) Tension b) Compression

No measurements of change in cross-section area was performed during the tests. The deformation of the specimen was visually observed to be rather homogeneous, however, in both tension and compression during most of the test. Therefore, nominal stress and strains will to some degree provide a measure for comparing the response of the specimen in test and simulations. Such curves are presented in Fig. 5. These curves are based on the force-displacement data logged during the tests or determined with LS-DYNA, and the original cross-section area and gauge section length, respectively, were applied when calculating the stress and strain.

The two stress-strain curves in tension are very close to each other in Fig. 5, indicating that Boyce's model represent the observed behavior well. The model also accounts for the pressure sensitivity, as the yield stress in compression is found to be about twice as large as in tension in both tests and simulations. Still, the response in compression is stiffer in LS-DYNA than in the tests. A more careful calibration of the coefficients presented in Table 1 may provide a closer agreement. Another idea is to include more terms in the model. In particular, Boyce et al. (2000) proposed to introduce a dashpot element also in part B of the mechanistic model shown in Fig. 1.

The intention of this second dashpot was to represent a strain-induced crystallization effect occurring at rather large deformations when the chains straighten out. A further investigation of this extension of the model is a possible subject for future research.

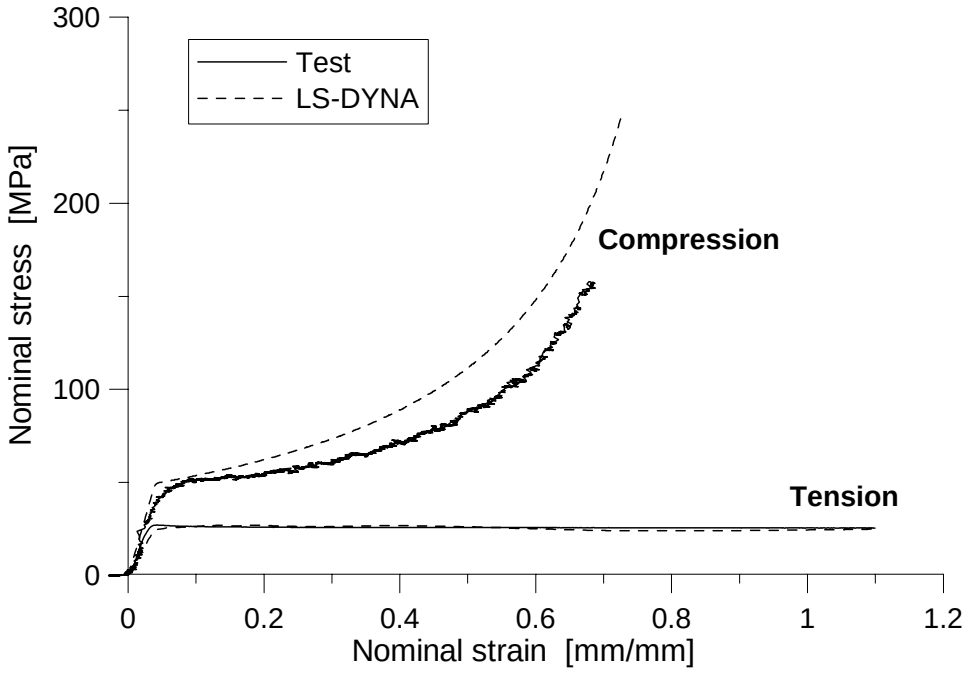

Figure 5: Nominal stress-strain curves from laboratory tests and LS-DYNA simulations

The deformed tension test specimen as calculated in the LS-DYNA simulation is shown in Fig. 6. Although the force oscillates slightly, see Fig. 4a), the specimen experiences a rather uniformous deformation in a similar way as observed in the laboratory test. Clearly, the model is able to distribute the deformation over the entire gauge length of the specimen, thereby avoiding localization. The cold drawing effect observed in the tests is thus fairly well predicted by the proposed model.

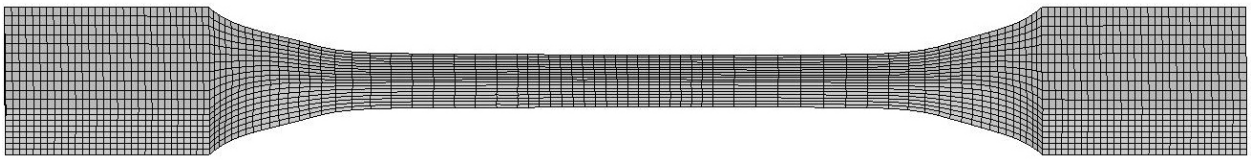

Figure 6: Deformed tensile specimen. LS-DYNA prediction.

Concluding Remarks

This paper presented an implementation of a constitutive model for thermoplastics in LS-DYNA. The model is based on earlier work by Professor Boyce's group at MIT, but a different approach for handling large elastic deformations is applied here. The model was checked by comparing results from uniaxial laboratory tests in tension and compression on polypropylene BA212 with predictions from LS-DYNA, and the agreement is at the current state of research promising. The model represents quantitatively the response in both loading modes, and, in particular, LS-DYNA gives a rather accurate estimate of the pressure sensitivity of yielding and the nominal stress-strain relationship in tension.

References

Argon AS: "A theory for the low-temperature plastic deformation of glassy polymers". *Philosophical Magazine*, **28**, 839-865 (1973).

Arruda EM and Boyce MC: "A three-dimensional constitutive model for the large stretch behavior of rubber elastic materials". *Journal of the Mechanics and Physics of Solids*, **41**, 389-412 (1993).

Boyce MC, Parks DM and Argon AS: "Large inelastic deformation of glassy polymers. Part I: Rate dependent constitutive model". *Mechanics of Materials*, **7**, 15-33 (1988).

Boyce MC, Socrate C and Llana PG: "Constitutive model for the finite deformation stress-strain behavior of poly(ethylene terephthalate) above the glass transition". *Polymer*, **41**, 2183-2201 (2000).

Buckley CP and Jones DC: "Glass-rubber constitutive model for amorphous polymers near the glass transition". *Polymer*, **36**, 3301-3312 (1995).

McCrum NG, Buckely CP and Bucknall CB: "*Principles of Polymer Engineering*". Oxford Science Publications (1997).

Haward RN and Thackray G: "The use of a mathematical model to describe isothermal stress-strain curves in glassy thermoplastics". *Proc Roy Soc A*, **302**, 453-472 (1968).

Meijer HEH and Govaert LE: "Mechanical performance of polymer systems: The relation between structure and properties". *Progress in Polymer Science*, **30**, 915-938 (2005).

Mills N: "*Plastics. Microstructure and Engineering Applications*". Butterworth-Heinemann (2005).

Moran B, Ortiz M and Shih CF: "Formulation of implicit finite element methods for multiplicative finite deformation plasticity". *Int J for Num Methods in Engineering*, **29**, 483-514 (1990).